

Light Metals 2012

**ALUMINUM ALLOYS:
Fabrication, Characterization
and Applications**

Material Characterization

SESSION CHAIR

Yansheng Liu

Secat, LLC

Lexington, Kentucky, USA

STUDIES ON FLOW CHARACTERISTICS AT HIGH-PRESSURE DIE-CASTING

Christian. M. Chimani¹, Richard Kretz¹, Simon Schneiderbauer², Stefan Puttinger², Stefan Pirker²

¹LKR Leichtmetallkompetenzzentrum Ranshofen GmbH, Austrian Institute of Technology, Postfach 26, 5282 Ranshofen, Austria

²Christian Doppler Laboratory on Particulate Flow Modelling, Johannes Kepler University, Altenbergerstr. 69, 4040 Linz, Austria

Keywords: High Pressure Die Casting, atomized flow; VOF modeling, water modeling

Abstract

The flow and filling characteristics influence product quality of high pressure die castings. A planar jet of liquid aluminum is formed at the ingate due to its high inlet velocity. The ingate design triggers the flow characteristics of the jet. Analytical investigations show that the process of drop formation at the liquid planar free jet is dominated by atomization at the ingate. Numerically, high-pressure die casting is attacked by a Volume of Fluid approach. Drop formation at the phase interphase cannot be captured by the numerical model since drops are much smaller than feasible grid spacing. Global spreading of the free jet in the casting mold is well pictured by this first numerical simulation. Experimentally the process is studied by water modeling validating the numerical results. The observed flow characteristics are discussed in comparison to product quality results observed in Al pressure die casting parts of the similar design.

Introduction

Due to its advanced degree of automation and its high productivity the high-pressure die-casting process is commercially the dominant technique for the production of die casting parts, for example, transmission housings, engine blocks and even small components like brackets, oil pump cases and water pumps.

Two main difficulties arising during the casting process are considered. Due to the high casting speed a free jet is formed at the ingate. At the surface of the jet droplets of liquid aluminum are formed. Depending on the shear forces between jet and the surrounding gas the jet disintegrates or atomizes, as discussed earlier in [10]. However, both lead to an increase of the surface ratio for the liquid aluminum, where oxidation may start. One the one hand, the collision of two disintegrated parts of the oxidized aluminum jet may cause cold runs. One the other hand, a high degree of atomization may increase the porosity of the final casting.

The influence of process parameters on the physics of high-pressure die-casting is not fully understood so far. This paper presents analytical, experimental and numerical investigations of this free jet to improve the understanding of high-pressure die-casting.

Analytical Considerations

A free jet can be characterized by the following dimensionless numbers

$$Re = \frac{\rho_l u d}{\mu_l}, We = \frac{\rho_l u^2 d}{\sigma_l} \text{ and } Oh = \frac{\mu_l}{\sqrt{\rho_l \sigma_l d}} = \frac{\sqrt{We}}{Re}, \quad (1)$$

where ρ_l , μ_l and σ_l denote the density, the molecular viscosity and the surface tension with respect to air of liquid aluminum, respectively. u is the velocity of the liquid jet at the ingate and d the width of the ingate. In equation (1) Re denotes the Reynolds number, which gives a measure of the ratio of inertial to viscous

forces. We is the Weber number describing the relative importance of the inertia of the fluid compared to the surface tension of the fluid. The Ohnesorge number Oh , which can be written in terms of Re and We , relates the viscous forces to inertial and surface tension forces. Note that a free jet is characterized explicitly by either specifying Re/We or Re/Oh (compare with equation (1)). In table 1 the calculated values of Re , We and Oh for typical inlet velocities of a planar jet of liquid aluminum with an ingate width of $d = 10^{-3}$ m are given.

Table 1. Re , We and Oh with $d = 10^{-3}$ m for different average velocities of the jet at the ingate u_n (properties of liquid aluminum $\rho_l = 2360 \text{ kg m}^{-3}$, $\mu_l = 0.00114 \text{ kg m}^{-1} \text{ s}^{-1}$, $\sigma_l = 0.86 \text{ N m}^{-1}$)

$u_n \text{ (m s}^{-1}\text{)}$	$Re \text{ (}\times 10^3\text{)}$	$We \text{ (}\times 10^3\text{)}$	$Oh \text{ (}\times 10^{-6}\text{)}$
30	57.8	2.3	830
60	116	9.2	830

[5] claim such a spray is composited into drops requiring energy. Due to the increase in surface during the formation of the drops the energy is proportional to the surface tension characterized, for example, by Oh . Furthermore, the necessary energy can be supplied by the nozzles or from shear forces acting on the spray [5]. Hence, the size and formation of these drops can be characterized by the Reynolds and Ohnesorge numbers, which divide the drop formation into three main regimes: (I) splattering, (II) wavy disintegration, (III) atomization (figure 1). Figure 1 shows that depending on the casting speed the free jet is either located in the wavy disintegration regime or in the atomization regime in case of high pressure die casting (compare with table 1). One the one hand, wavy disintegration of such a jet can inevitably lead to cold runs in the final casting. On the other hand, a high degree of atomization may strongly increase the porosity of the casting part.

Spray decay affects the casting process only if the distance between the nozzle and the onset of drop formation is greater than the spatial dimensions of the casting mold. By an experimental investigation of a planar free jet it is found in [11] that the distance between nozzle and the onset of drop formation is given by

$$x_i = 7560 \Lambda We_{\Lambda}^{-0.74} \text{ with } \Lambda = \frac{d}{4}, \quad (2)$$

which is valid over a broad range of Weber numbers. The corresponding Sauter mean diameter SMD_i at x_i was determined to comply [11]

$$SMD_i = 134 \Lambda We_{\Lambda}^{-0.76}, \quad (3)$$

which is a common measure of the mean particle diameter. Table 2 shows that drop formation starts immediately (between $5d$ and $16d$) as the fluid leaves the nozzle for the sprays specified in table 1. The calculated values for x_i and SMD_i and figure 1 suggest that at $u_n = 60 \text{ m s}^{-1}$ the spray is highly atomized and at $u_n = 30 \text{ m s}^{-1}$ $250 \mu\text{m}$ drops are formed from surface waves

Table 2. Onset of drop formation (equation (2)) and Sauter mean diameter (equation (3)) for different average velocities of the jet at the ingate u_{in} .

u_{in} (m s ⁻¹)	x_i (10 ⁻³ m)	SMD_i (10 ⁻⁶ m)
30	16	249
60	5.7	87

Additionally, the onset of drop formation, i.e. the regime of the spray decay, can be influenced by the nozzle geometry near regime transitions. This implies that in case of $u_{in} = 60 \text{ m s}^{-1}$ atomization may be minimized by utilizing an appropriate nozzle. In figure 2 sketches of inflow profiles of a free jet for different types of nozzles are shown. Since the velocity gradient at the surface of liquid jet is important for the formation of drops the Weber number should be calculated based on the velocity at $d/2$ (figure 2). Hence, utilizing a pipe nozzle instead of a smooth contraction nozzle (assumed in table 1) can significantly reduce atomization. In contrast, orifice nozzles may amplify atomization. Finally, in case of $u_{in} = 30 \text{ m s}^{-1}$ utilizing an orifice nozzle may cause a transition from wavy disintegration to atomization.

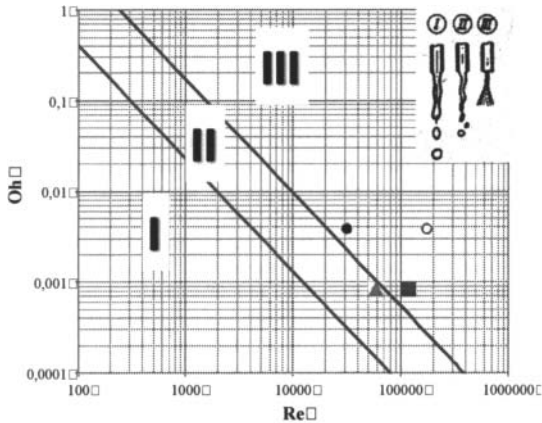


Figure 1. Graph of drop decay processes according to [5] (I: splattering, II: wavy disintegration, III: atomization) with schematic representation from [7]. The triangle corresponds to the planar free jet with $u_{in} = 30 \text{ m s}^{-1}$ and the rectangle to $u_{in} = 60 \text{ m s}^{-1}$. The filled and empty circle indicate the experiments performed with water with $p = 0.4 \text{ MPa}$ and $p = 1.2 \text{ MPa}$, respectively.

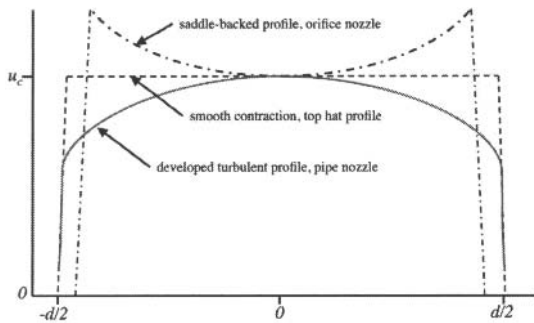


Figure 2. Sketches of initial velocity profiles from a sharp edged orifice nozzle, a smooth contraction nozzle and a long pipe for a round jet (from [3]).

Experimental investigation of influence of nozzle geometry

In order to support the conclusions drawn with respect to the nozzle geometry in the previous section we investigated a free jet of water for two different nozzles (figure 3) experimentally using a high-speed camera. To this end, the velocity at the nozzle and the nozzle diameter were chosen so that the spray of water was located slightly above the transition between wavy disintegration and atomization (filled circle figure 1). Additionally, a second, higher velocity at the nozzle outlet was examined to study the influence of the nozzle geometry in different regimes of the spray decay.



Figure 3. Sketch of the experimental setup: orifice nozzle ($d = 10^{-3} \text{ m}$) left and pipe nozzle ($d = 10^{-3} \text{ m}$) right hand side

In figures 4 and 5 the influence of the nozzle geometry on the free jet of water is shown for both values of the velocity at the nozzle outflow. Figure 4 indicates that the slower free jet disintegrates by surface waves in case of the pipe nozzle and slightly atomizes in case of the orifice nozzle ($x_i = 3.6 \text{ mm}$, $SMD_i = 25 \mu\text{m}$). Note that the mean droplet diameter is smaller than the maximum resolution ($r = 0.1 \text{ mm}$) of the high-speed camera at the necessary frame rate of 15000 frames per second. Hence, the dilute atomization observed in the experiment is not detected in the photograph. Remarkably, the analytical predictions are verified by the experiment. Finally, in figure 5 photographs of the higher speed of the free jet of water are shown ($x_i = 0.4 \text{ mm}$, $SMD_i = 2 \mu\text{m}$). It can be found from the figure that in the highly atomized regime the geometry of the nozzle does not lead to a regime transition but affects the degree of atomization.

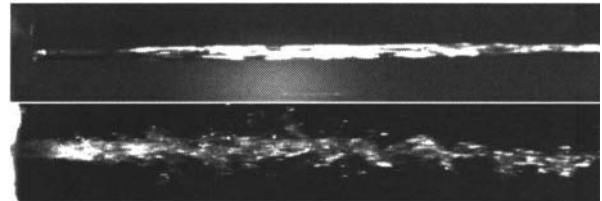


Figure 4. Free jet of water with $p_{in} = 0.4 \text{ MPa}$. Top: orifice nozzle; bottom: pipe nozzle (horizontal dimensions 0.06 m)

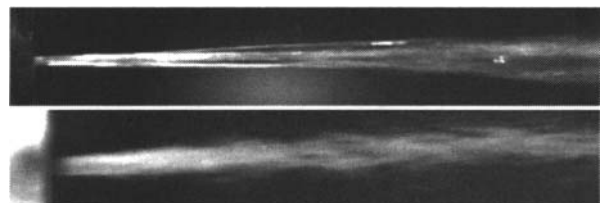


Figure 5. Free jet of water with $p_{in} = 1.2 \text{ MPa}$. Top: orifice nozzle; bottom: pipe nozzle (horizontal dimensions 0.06 m).

Numerical simulation of high pressure die casting

Besides the analytical and experimental investigation of the planar liquid jet the feasibility of the numerical simulation of the casting

process was studied. The two phase fluid flow is modeled by an volume of fluid model (VOF) [1]. On the one hand, a large eddy (LES) turbulence requiring high grid resolutions is tested. On the other hand, we checked whether an unsteady Reynolds averaged turbulence model (URANS) is able to picture the global behavior of the free jet adequately. However, while it is expected that the LES simulation is able to model the free jet, LES simulations may be infeasible with respect to computational resources. The simulation parameters for both are given in table 3. The dimensions of the stair-step shaped casting mold are indicated in figures 6 and 7. The width of the casting was 0.014 m at the ingate, the depth 0.1 m and the height 0.18 m. The ingate width was $d = 0.001$ m and the velocity at the ingate was chosen 60 m s^{-1} .

In figure 6 the results obtained by the LES and by the URANS simulation are shown. Surprisingly, although the grid spacing used in the LES simulation is approximately one third of that in the URANS simulation, both models lead to a similar global distribution of the liquid aluminum. I.e. the free jet collides with the walls of the casting mold at the second step for $t < 15$ ms and the free jet pushed towards the first step for $t > 15$ ms. Above the second step the coarser grid resolution of the URANS model is reflected in the wider spreading of the jet. However, even the grid resolution used in the LES simulation is not sufficient to capture the drop formation at the interphase since the drops are an order of magnitude smaller. Hence, sub-models would be required to model drop formation in both cases. Additionally, the LES simulation requires approximately 30 times more computational resources than the URANS simulation.

Table 3. Numerical settings for the VOF simulation of high-pressure die-casting. For details about the numerical schemes the reader is referred to [1].

	LES	URANS
Turbulence	Smagorinsky	$k-k_r-\omega$
Surface tension	Yes	Yes
Pressure	PRESTO!	PRESTO!
	Central	Second order
Momentum	Differencing	upwind
VOF	CICSAM	Geo-reconstruction
# cells	950400	47040

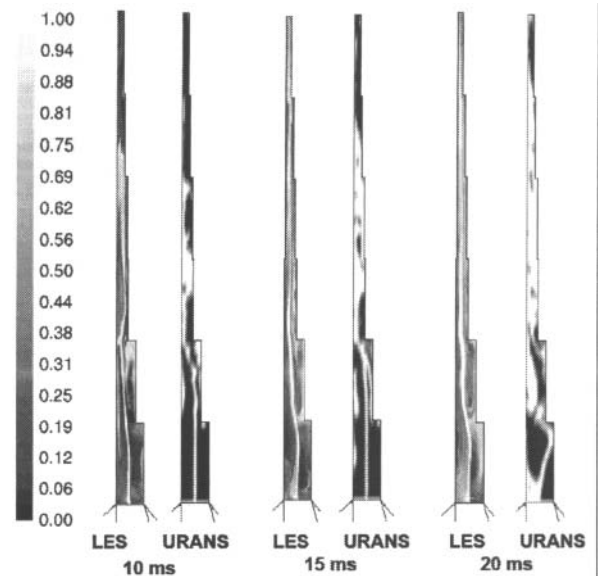


Figure 6. Volume fraction of liquid aluminum α at the symmetry plane

Additionally, we have implemented a cold run detection algorithm. As mentioned in the introductions cold runs may appear if at least two oxidized fronts of liquid aluminum collide. Preferentially, cold runs are located near the wall of the casting mold. Hence, numerically such a collision corresponds to the positive flux of liquid aluminum through at least two opposite side faces into a grid cell. In figure 7 the cold runs (in red) detected in the numerical simulation are shown. Most of the cold runs are located at the second step, where the jet initially collides with the casting mold. Visual comparison with the disintegrated free jet (figure 7) shows that this algorithm adequately detects such colliding fronts of liquid aluminum.

To conclude, high-pressure die-casting can be investigated numerically by utilizing URANS turbulence models. Increasing the grid resolution and increasing the degree of the resolved unsteady dynamics, i.e. LES, does not significantly improve the understanding of the industrial process. The resolution URANS model is also sufficient to detect cold runs and to study the influence of the main process parameters. However, resolving drop formation seems to be unfeasible using a VOF approach since it would require approximately two orders of magnitude more computational resources.

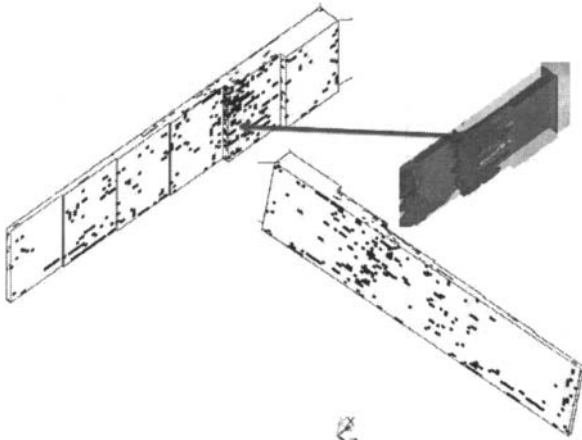


Figure 7. Detected cold runs (= black) by the URANS simulation. The top right figure indicates the volume filled with liquid aluminum at $t \approx 10$ ms

Experimental simulation of high pressure die casting

To experimentally study the jet formation, as well as the filling behavior a water model of the process has been set up. The step-plate shaped mold as discussed in the numerical part was rebuilt as transparent Acryl plastic mold and mounted to a UBE HVSC 350 Squeeze Casting machine. The casting parameter setup corresponds with high pressure die casting conditions as given in the previous chapter.

To account for comparability of experimental water modeling to the expected flow behavior of liquid Al the process parameters were chosen to achieve comparable Reynolds numbers at similar average inlet velocity at the nozzle exit, which leads to a aim water temperature of 80°C for the experiment.

High-speed movies have been recorded with a Photron Fastcam SA3 camera at 5000 and 10000 fps and very low exposure times from 5 to 100s per frame to reduce motion blurring. To achieve sufficient illumination three studio spotlights with 1300W each have been used. Camera distance to the casting mold was approx. 0.3m. The camera orientation was parallel to the steps and perpendicular to the narrow side of the plate. Thus the images provide information on the flow characteristics primarily determined by the flow close to the narrow face of the plate like mold. As the average droplet size is of a view microns only it was not feasible to detect individual droplets nevertheless the general flow characteristics are observable.

Figure 8 provides a detailed view close to the inlet nozzle at the bottom left side of the picture up to the first two steps of the mold cavity 0.002s after start of water injection. The picture clearly indicates the immediate atomization of the free jet as predicted analytically and by numerical simulation. The major part of the jet is guided by the left side wall of the mold while the right side is disperses and collides at the mold wall at the corner of the first step. It must be mentioned that this results deviate compared to the flow characteristic provided by numerical simulation predicting the free jet at the left side of the mold for a longer distance. The reason for this mismatch must be contributed to a machining discrepancy to the corresponding numerical model that leads to an inlet nozzle position shifted by 5mm to the left side plate of the mold.

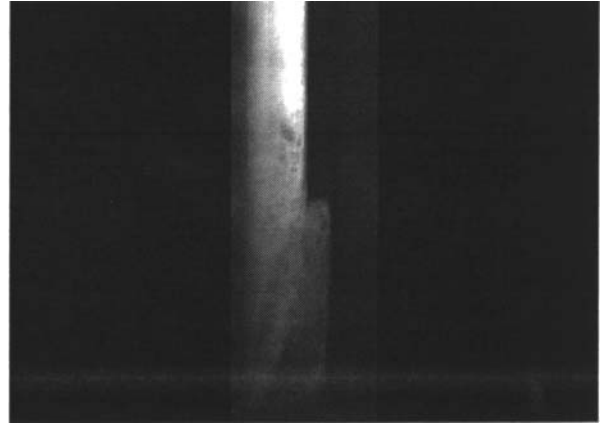


Figure 8. High speed camera picture 0.002s after start of injection. Detail of the first two steps of the mold corresponding to 0.08m.

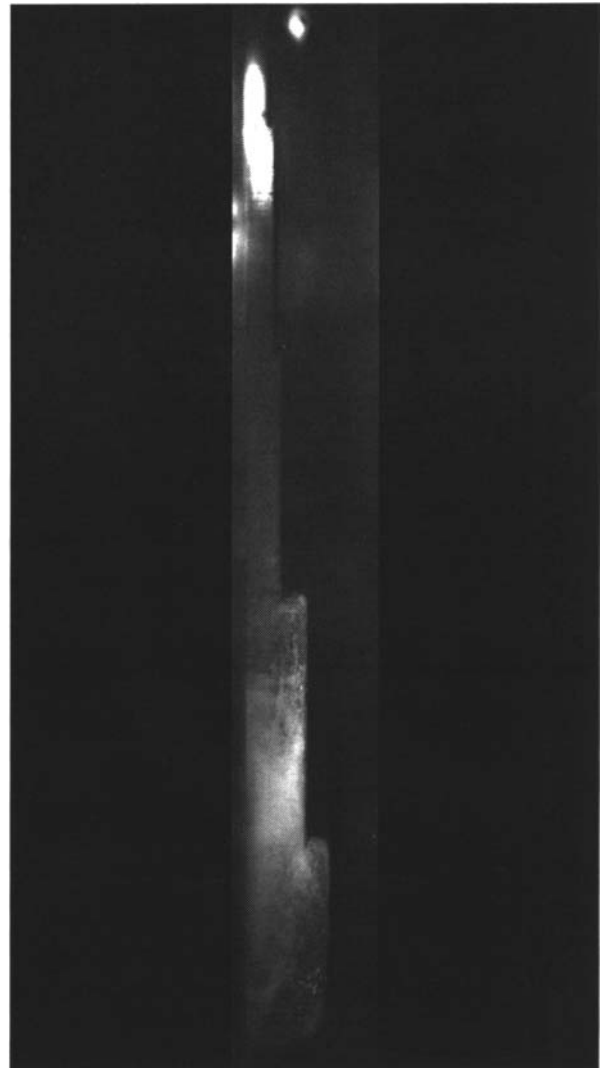


Figure 8. High speed camera picture 0.006s after start of injection. Narrow face view of the stair-step shaped mold cavity

The major volume fraction of the atomized jet impinges at the top end of the mold, leading to a top-down filling flow at the end of the process as predicted numerically. Figure 9 provides a narrow face view of the mold cavity 0.006s after start of injection. leading to a top down filling

Conclusions

In this paper, the flow and filling characteristics during injection of liquid aluminum during high pressure die casting has been studied threefoldly: a) analytically, b) experimentally and c) numerically. It has been shown analytically and experimentally that the geometry of the nozzle at the ingate significantly influences the process of the drop formation at the surface of the free jet of liquid aluminum. Numerically, the drop formation cannot be resolved with an acceptable computational effort. However, the simulation of high-pressure die-casting delivers an appropriate measure of the casting process and is able to predict cold runs.

The feasibility of water modeling to experimentally simulate the high pressure die casting process has been introduced providing the basis to validate numerical models.

To conclude, this paper leads to a better understanding of this challenging casting technique. The presented scientific findings introduce investigation techniques enabling casting professionals to optimize their casting products depending on the special demands on the final casting.

Acknowledgement

The authors would like to thank for supporting this R&D project by the Federal Ministry for Transport, Innovation and Technology (Bmvi) and by the province of Upper Austria

References

1. Ansys Inc *Ansys Fluent 12.0 Theory Guide* (User Manual 2009)
2. Dai Z, Chou W-H and Faeth G, "Drop formation due to turbulent primary breakup at the free surface of plane liquid wall jets" *Phys. Fluids*, 1998, no. 10:1147–57
3. Deo R C, "*Experimental investigations of the influence of Reynolds number and boundary conditions in a plane air jet*" (PhD thesis, University of Adelaide, Australia), 2005
4. Faghani E, et. al., "Numerical investigation of turbulent free jet flows issuing from rectangular nozzles: the influence of small aspect ratio", *Arch. Appl. Mech.*, no. 80, 727–45
5. Ohnesorge W v, *ZAMM*, 1936, no16: 335
6. Lee K-H, Setoguchi T, Matsuo S and Kim H-D, "Influence of the nozzle inlet configuration on under-expanded swirling jet" *Proc. IMechE G: J. Aerospace Engineering*, 2006, no 220: 155–63
7. Prandtl L, Osawtitsch K and Wieghardt K, „*Führer durch die Strömungslehre*“ (Braunschweig: Vieweg), 1993, ed. 9,
8. Sallam K A, , et. al., "Drop formation at the surface of plane turbulent liquid jets in still gases", *Int. J. Multiphase Flow*, 1999, no. 25, 1161–80
9. Sallam K A, Dai Z and Faeth G M, "Liquid breakup at the surface of trubulent round liquid jets in still gases", *Int. J. Multiphase Flow*, 2002, , no. 28, 427–49
10. Schneiderbauer S. , et. al., "Studies on Flow Characteristics at High Pressure Die Casting", Proceedings, ICASP 3rd International Conference on Advances in Solidification Processes, 2011
- 11 Wu P K and Faeth G M, "Onset and end of drop formation along the surface of turbulent liquid jets in still gases" *Phys. Fluids*, 2005, A 2, 2915–19